https://doi.org/10.14669/AM/210423

CAR PLATOONING STRING STABILITY ANALYSIS FOR AUTOMATIC LONGITUDINAL CONTROL IN AUTOMATED HIGHWAY SYSTEMS

LICH DUC LUU[1], NGUYEN HUU HIEU[2], QUOC THAI PHAM[3], NGO SY DONG[4]

Abstract

Forming car platoons and managing them through automation allows cars to travel with shorter gaps, which contributes to increasing road throughput, lowering fuel use, and cutting emissions. However, minimizing inter-vehicle spacing must comply with the principle of string stability. This paper introduces a Linear Quadratic Integral Regulator (LQIR) tailored for the Adaptive Cruise Control (ACC) strategy within a platoon of vehicles. The regulator integrates two additional states to guarantee both effective tracking and preservation of string stability. Furthermore, a heuristic procedure is proposed to select the Constant Time Headway Policy (CTHP) as a means of achieving stability. The selection routine combines an examination of the magnitude frequency response with an inspection of the pole–zero distribution of the spacing-error transfer function between successive vehicles. Using this approach, a comparative investigation is carried out for two autonomous ACC architectures: one based on absolute position feedback and another on measured inter-vehicle distance.

Keywords: string stability; vehicle platoon; adaptive cruise control; LQIR; spacing policy

[1] Faculty of Transportation Mechanical Engineering, The University of Danang - University of Science and Technology, 54 Nguyen Luong Bang, Da Nang 550000, Vietnam, e-mail: ldlich@dut.udn.vn, ORCID: 0000-0001-5612-5126

[2] Faculty of Electrical Engineering, the University of Danang - University of Science and Technology 54 Nguyen Luong Bang St., Lien Chieu, Danang, Viet, 550000, 550000, Vietnam, e-mail: nhhieu@dut.udn.vn, ORCID: 0000-0001-9538-7663

[3] Faculty of Transportation Mechanical Engineering,, The University of Danang - University of Science and Technology, 54 Nguyen Luong Bang, Da Nang 550000, Vietnam, e-mail: pqthai@dut.udn.vn, ORCID: 0000-0003-4783-2659

[4] Faculty of Mechanical - Automotive and Civil Engineering, Electric Power University, 100000, Ha Noi, Vietnam, e-mail: dongns@epu.edu.vn, ORCID: 0009-0009-8478-4845

https://doi.org/10.14669/AM/210423

1. Introduction

Automated car platoons are a crucial part of intelligent transportation systems [1] that represent a promising approach to improve highway efficiency or dedicated lane(s). Autonomous car control aims to enhance driver safety and decrease accident rates by removing driver intervention from the driving system [2]. Fully automated cruise control systems have become an integral part of modern highway designs, with a focus on improving traffic flow and overall freeway efficiency [3, 4].

Recently, ACC systems have become a common feature in passenger cars today. Instead of the driver needing to frequently adjust the throttle and brake pedals, the ACC system can assume control of the car based on the driver's selected speed. Thus, this system also provides the advantage of mitigating driver fatigue during extended trips [5]. These technologies utilize built-in sensors—most commonly radar—to detect both the speed difference and the gap between the car and the one ahead. The collected data is subsequently processed by a control system, which adjusts the throttle or brake of the subject car as needed. The ACC is introduced as an enhanced iteration of the traditional cruise control (CC) system [6, 7, 8]. Recent experimental results [9] and reports [10] suggest that commercially deployed ACC systems do not achieve string stable, highlighting the need for further research on advanced ACC systems.

Two properties of the ACC platoon are important: Individual car stability, which is the perturbations converges to zero for all followers, and string stability [11], which implies that disturbances on the leading car do not undergo amplification as they propagate downstream. However individual car stability is easily achieved. The current research focuses on the well-known ACC technology, a driver assistance system created to maintain a desired spacing by adjusting the car's velocity based on the changes in the velocity of the lead car [12, 13]. The interdependence of string stability and spacing policies is a crucial consideration in the design of an ACC system controller. String stability and spacing policy are mutually binding, which can be found in [14]. String stability is generally interpreted as the property of interconnected systems to remain asymptotically stable [15]. For the ACC platoons, the authors of [16] proposed evaluating string stability using the infinity norm of the transfer function that describes how distance errors propagate. Meanwhile, [17] presented a practical method that accounts for time delays and dynamic lags inherent in car longitudinal motion. Several alternative methodologies for analyzing string stability have also been outlined in [18] and [19].

The objective of this study is to create a LQIR for ACC cars in a platoon, ensuring both good performance and string stability. To achieve the desired performance, a dual integrations is added to the controller, while string stability is ensured by choosing the CTHP through a novel heuristic approach, addressing the stability conditions mentioned in [15]. This approach involves determining the transfer function for spacing errors for two consecutive cars. Subsequently, the stability of the platoon is assessed for two ACC configurations: one

https://doi.org/10.14669/AM/210423

based on location and the other based on spacing. Using the plot displays the frequency response of spacing errors transfer functions, a solution for string stability among inter-connected cars has been developed. This solution enables the selection of CTHP to satisfy the first stability condition as proposed by [15]. To satisfy the second stability requirement, the constant time headway parameter is further increased, and the pole–zero distribution of the spacing-error transfer function is examined. From this analysis, an updated value of the CTHP is obtained following the criterion discussed in [15]. Subsequently, simulation experiments are carried out to confirm the effectiveness of the proposed heuristic method in guaranteeing string stability.

This study is organized as follows: In Section 2, we first consider the modeling of cars. The adaptive cruise control design approach is presented in Section 3. In Section 4, the stability analysis of the car platoon is presented. In Section 5, the performance validation is implemented and in Section 6, conclusions will close this study.

2. Methods

2.1. Modeling of Car

The car's dynamics is represented by a nonlinear model that incorporates various factors such as the powertrain, aerodynamics drag road, tyre resistance and gravity. Nonlinear car dynamics pose challenges for platoon design, requiring simplified models. In [21], a linearized model for car longitudinal dynamics is introduced. Describing the balance of forces acting on the car's longitudinal axis, Newton's second law can be expressed as follows:

$$\dot{\bar{v}}_x(t) = \frac{1}{m_v}(\bar{P}_x - R_a - R_G - R_x), \tag{1}$$

here, $\bar{v}_x$ represent longitudinal speed of the car, v_w is the wind velocity, m_v is the car mass, $\bar{P}_x$ is the longitudinal tyre force, $R_a = 0.5\rho_v S_v A_v(\bar{v}_x + v_w)^2$ is the force due to aerodynamic drag with ρ_v being the air density, A_v representing the car frontal area and S_v representing the drag coefficient of the car. The gravitational force component is represented by $R_G = m_v g sin\bar{\beta}$ with $\bar{\beta}$ representing the road slope. $R_x = C_R m_v g cos\bar{\beta}$ is the force due to rolling resistance at the wheels with C_R representing the modified resistance coefficient to take account of cornering resistances.

The equation above exhibits nonlinearity concerning the longitudinal velocity of the car $\bar{v}_x$, linearization can be achieved by employing a first-order Taylor approximation around the equilibrium point v_0, P_0, β_0. At equilibrium at $d\bar{v}_x / dt = 0$, Eq. 1 can be solved for:

$$P_0 = \frac{1}{2}\rho_v A_v S_v (v_0 + v_w)^2 + C_R mg\cos\beta_0 + m_v g\sin\beta_0, \tag{2}$$

https://doi.org/10.14669/AM/210423

where P_0 can be determined by assuming appropriate values for $v_0, \beta_0, C_R, A_v, S_v, v_w, \rho_v$. The linearized model can be expressed as follows:

$$\begin{aligned} &\varsigma_v \dot{v} + v = K_v(u + \lambda) \\ &\dot{v} = -\frac{1}{\varsigma_v} v + \frac{K_v}{\varsigma_v}(u + \lambda), \end{aligned} \tag{3}$$

where the perturbed variables are defined as: $\overline{v}_x = v - v_0$, $u = \overline{P}_x - P_0$, $\beta = \overline{\beta} - \beta_0$. The parameters ς_v, K_v and λ are defined as follows (see in [21]):

$$\begin{aligned} &\varsigma_v = m_v / (\rho_v S_v C_v (v + v_w)^2) \\ &K_v = 1 / (\rho_v S_v C_v (v + v_w)^2) \\ &\lambda = m_v g (C_R \sin\beta_0 - \cos\beta_0)\beta. \end{aligned} \tag{4}$$

The car model depicted in Figure 1 was constructed using the linearized equations and can be expressed in the form of a transfer function.

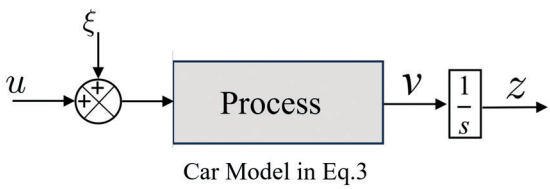

Fig. 1. Block diagram of linearized car longitudinal dynamics

2.2. ACC design method

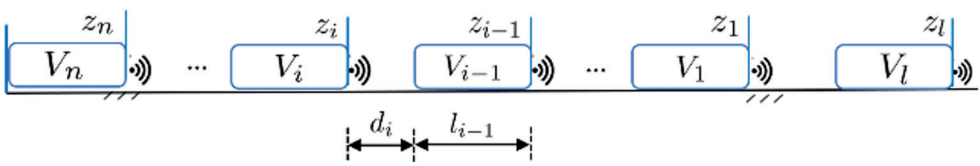

Fig. 2. Car platooning with the ACC system

Figure 2 illustrates the structure of a car platoon, which consists of one lead car followed by n trailing cars. For analysis, it is assumed that the entire platoon travels from left to right. The location of the i^{th} car, measured from a fixed roadside reference point (0), is represented

https://doi.org/10.14669/AM/210423

as z_i. The separation between each pair of adjacent cars, as detected by onboard sensors, is denoted by d_i, while l_i refers to the length of the car.

The leading car employs a cruise control (CC) system implemented with a proportional–integral (PI) controller based on the formulation in Eq. 2. Each following car in the platoon uses an ACC strategy to maintain the appropriate spacing between itself and the car directly ahead. The primary goal of these controllers is to ensure that every car consistently keeps a target gap from its predecessor, as specified by CTHP:

$$D_{i,ref} = r_0 + b_i v_i . \tag{5}$$

In this context, r_0 denotes the minimum spacing required when cars are stationary, while b_i indicates the time headway assigned to the ith car. As each car accelerates, the location z_{i-1} of the preceding car introduces a parabolic disturbance. To address this, the ACC controller must incorporate dual integrators to successfully mitigate such disturbances. Because of this requirement, traditional PID controllers are unsuitable, and a LQR with dual integrations – referred to as LQI²R – is selected instead. The design of the LQI²R controller necessitates an augmented plant model with two integrators, applicable for both types of ACC configurations: those based on absolute position and those based on inter-car spacing.

2.2.1. ACC cars Control Structure based on Location

The distance error of the car i with respect to the car i–1 in scenarios of [15] is defined as:

$$\delta_{iz}(t) = z_{i-1} - z_i - (l_{i-1} + D_i) = z_{i-1} - z_i - D_{i,ref} , \tag{6}$$

where $D_{i,ref}$ is the desired distance for two consecutive cars, consisting of the length l_{i-1} of the preceding car.

The ACC configuration based on location with the desired spacing Eq. 6 is described in [22] $z_{i,ref} = z_{i-1} - r_0$ as a reference and $y_{iz} = z_i - b_i v_i$ as an output signal, is denoted in Figure 3. Considering the desired spacing Eq. 6, the control error, as expressed in equation Eq. 6, is obtained.

$$\delta_{iz}(t) = z_{i-1} - r_0 - (z_i + b_i v_i). \tag{7}$$

The ACC configuration does not rely on information from the measuring device and may not be implemented, as the location z_{i-1} of the preceding car is unknown. To address this limitation, the ACC structure can be reconfigured, resulting in an equivalent control structure as shown in Figure 3. This reconfigured structure can effectively utilize the radar sensor measurement and is suitable for implementation.

https://doi.org/10.14669/AM/210423

It is important to highlight that in Figure 4, r_0 does not act as a reference signal. The control error is still defined according to Eq. 7, while the position z_{i-1} of the preceding car is regarded as an external disturbance.

To capture this behavior, the car's extended state-space representation is constructed by enhancing the model in Eq. 3 with two additional integrators inserted into the error channel.

$$\begin{cases} \dot{x}_{1z} = \dot{z}_i = \dot{v}_i \\ \dot{x}_{2z} = \dot{v}_i = -\dfrac{1}{\varsigma_v} v_i + \dfrac{K_v}{\varsigma_v}(u_{iz} + \lambda_i) \\ \dot{x}_{3z} = \delta_{iz} \\ \dot{x}_{4z} = x_{3z} \\ y_{iz} = z_i + b_i v_i \end{cases}, \tag{8}$$

$$\Rightarrow \begin{cases} \dot{x}_{iz} = A_{iz} x_{iz} + b_{iz} u_{iz} \\ y_{iz} = C_{iz}^T x_{iz} \end{cases}. \tag{9}$$

The LQI²R controller was chosen specifically to eliminate the parabolic disturbances caused by the location z_{i-1} of the car ahead. For the state-space model described in Eq. 9, the structure of the LQI²R controller is constructed as follows:

$$u_{iz} = -K_{iz} x_{iz} = k_{1z} v_i + k_{2z} D_i + k_{3z} \int \delta_{iz}(\tau) d\tau + k_{4z} \int (\int \delta_{iz}(\tau) d\tau) d\tau. \tag{10}$$

In this formulation, K_{iz} denotes the matrix of state feedback gains, with the coefficients K_{1z} through K_{4z} representing its individual elements. The state vector is defined as $x_{iz} = [x_{1z}, x_{2z}, x_{3z}, x_{4z}]^T$.

The optimization procedure entails computing the control input u_{iz} that minimizes a performance index $J_{u_{iz}}$. This index encompasses both the performance characteristic requirement and the limitations of controller input, typically expressed as:

$$J(x_{iz}, u_{iz}) = \int_0^\infty (x_{iz}^T Q x_{iz} + u_{iz}^T R u_{iz}) d\tau, \tag{11}$$

where $Q = Q^T \geq 0$ and $R = R^T \geq 0$ are positive determine weighting matrices. For obtaining a solution to the optimal controller provided by Eq. 10, it is essential that the linear time-invariant system is stabilizable, a condition satisfied by the system described by Eq. 9. According to linear optimal control theory, the gain K_{iz} that minimizes Eq. 11 has the following form:

$$K_{iz} = (P + b_{iz}^T R b_{iz})^{-1} b_{iz}^T R A_{iz}. \tag{12}$$

https://doi.org/10.14669/AM/210423

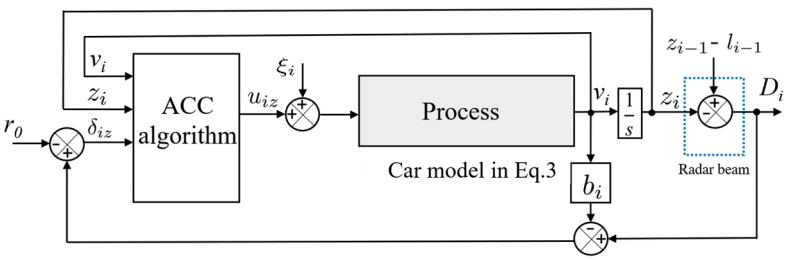

Fig. 3. Position-based ACC system for car structure

where the matrix P is the solution of the Algebraic Riccati Equation:

$$A_{iz}^T RA_{iz} - R + Q - A_{iz}^T Rb_{iz}(b_{iz}^T Rb_{iz} + P)^{-1} b_{iz}^T RA_{iz} = 0. \tag{13}$$

2.2.2. ACC Cars Control Structure based on Distance:

When the target spacing $D_{i,ref}$ is considered as the reference input and the actual spacing D_i, obtained from onboard sensors, is used as the controlled output, the system corresponds to the spacing-based ACC configuration described in [21] and illustrated in Figure 4. In this case, the control error is defined as:

$$\delta_{iD}(t) = D_{i,ref} - D_i = D_{i,ref} - (z_{i-1} - z_i). \tag{14}$$

The location z_{i-1} of the preceding car, which is not directly measured but instead introduced by radar (sensor), introduces a disturbance in the controlled system. To compensate for its negative effect, two integrators are introduced into the error channel, thereby yielding the extended state model:

$$\begin{cases} \dot{x}_{1D} = \dot{D}_i = v_{i-1} - v_i \\ \dot{x}_{2D} = \dot{v}_i = -\dfrac{1}{\varsigma_v} v_i + \dfrac{K_v}{\varsigma_v}(u_{iD} + \lambda_i) \\ \dot{x}_{3D} = \delta_{iD} \\ \dot{x}_{4D} = x_{3D} \\ y_{iD} = D_i \end{cases}, \tag{15}$$

$$\Rightarrow \begin{cases} \dot{x}_{iD} = A_{iD} x_{iD} + b_{iD} u_{iD} \\ y_{iD} = C_{iD}^T x_{iD} \end{cases}. \tag{16}$$

https://doi.org/10.14669/AM/210423

The inclusion of the two integrators in Eq. 16 is achieved in this ACC structure by selecting the LQI²R controller, which is described by:

$$u_{iD} = -K_{iD}x_{iD} = k_{iD}v_i + k_{2D}D_i + k_{3D}\int \delta_{iD}(\tau)d\tau + k_{4D}\int(\int \delta_{iD}(\tau)d\tau)d\tau. \tag{17}$$

Under this configuration, the error term δ_{iD} is defined according to Eq. 14, while the corresponding control signal u_{iD} is obtained by optimizing a cost function analogous to that in Eq. 11.

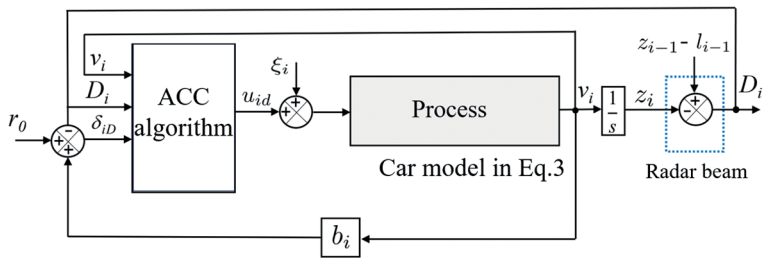

Fig. 4. Spacing–based ACC system for car structure

2.3. Stability analysis of car platoon

Because car platoons using ACC systems may be prone to string instability, it is essential to establish a method for evaluating platoon stability. Such a method enables the determination of whether the platoon remains stable or becomes unstable over time. This analysis focuses on the propagation of spacing errors within the ACC framework. A platoon is classified as string stable if these spacing errors do not grow larger as they move down the line of cars. Conversely, if instability is present, the magnitude of spacing errors increases from one car to the next, which can ultimately undermine platoon control and raise the risk of accidents or unsafe situations. Therefore, achieving string stability is fundamental to ensuring that the platoon operates in a safe and synchronized manner.

For both scenarios, the transfer functions representing the correlation between the spacing errors of two consecutive cars in the platoon will be defined as follows:

$$\Xi_i(s) = \frac{\delta_i(s)}{\delta_{i-1}(s)}, \tag{18}$$

let $\delta_i(s)$ be the Laplace transform of $\delta_i(t)$.

In the context of string stability, the condition of the spacing errors of two consecutive cars in the platoon can be expressed in the frequency domain as follows:

https://doi.org/10.14669/AM/210423

$$\|\delta_{i-1}\|_\infty \geq \|\delta_i\|_\infty \geq \ldots \geq \|\delta_n\|_\infty \qquad for\, i \geq 2. \tag{19}$$

This implies that the spacing error of two consecutive cars in the platoon should progressively decrease along the platoon, beginning from the first car following the leader. The stability condition Eq. 19 may be builded using the theory of linear systems, depending on the transfer function Eq. 18 and its impulse response $\Xi_i(s)$, following the relation $\|\delta_i\|_\infty \leq \|\Xi_i(t)\|_1 \|\delta_{i-1}\|_\infty$, where $\|\Xi_i(t)\|_1 = \int_0^\infty |\Xi_i(t)| dt$.

Accordingly, the necessary and sufficient requirement for string stability can be formulated as $\|\Xi_i(t)\|_1 \leq 1$. In [13], this condition was reformulated and expressed through the following equivalent relations:

$$\|\Xi_i(j\omega)\|_\infty \leq 1, \tag{20}$$

$$\Xi_i(t) > 1, \quad \forall t \geq 0. \tag{21}$$

The condition Eq. 20 ensures that $\|\delta_i\|_2 \geq \ldots \geq \|\delta_n\|_2$, this implies that the spacing errors decreases as they propagate towards the rear of the platoon [15]. Besides, a heuristic approach is introduced to analyze the stability of an autonomous car string in a platoon, with a specific focus on inequality Eq. 20. Ascending values of headway time ($b_i > 0$) are considered, and the corresponding frequency response of $\Xi_i(j\omega)$ is plotted, checking the condition $\Xi_i(j\omega)$ for $\omega > 0$ by testing the maximum magnitude of frequency response. if the maximum magnitude is less than 1, the string is considered stable since the inequality Eq. 20 is satisfied. Of particular interest is the minimum value of b_i for which the maximum magnitude is less than 1.

The condition Eq. 21 ensures that $\|\delta_i\|_\infty \geq \ldots \geq \|\delta_n\|_\infty$, and thus, the transfer function $\Xi_i(s)$ must satisfy two necessary conditions as given in [20] in order to fulfill condition Eq. 21:

- The leading poles of $\Xi_i(s)$ must not consist of a complex-conjugate pair, since such a configuration would generate oscillatory dynamics.
- In addition, no zeros of $\Xi_i(s)$ should appear to the right of all system poles on the complex plane.

To comply with condition Eq. 21 and achieve a reliable form of string stability, these two requirements are checked using the pole–zero map of the transfer function $\Xi_i(s)$. The procedure involves analyzing b_i values that exceed the minimum threshold already identified as fulfilling condition Eq. 20.

https://doi.org/10.14669/AM/210423

2.3.1. Stability analysis of ACC system based on location

Spacing error is initially considered:

$$\delta_{iz} = z_{i-1} - z_i - r_0 - b_i \dot{z}_i. \tag{22}$$

Differentiating the above equation yields:

$$\begin{aligned}
&\dot{\delta}_{iz} = v_{i-1} - v_i - b_i \dot{v}_i \Rightarrow \dot{z}_i = v_i = \dot{z}_{i-1} - \dot{\delta}_{iz} - b_i \ddot{z}_i \\
&\ddot{\delta}_{iz} = \dot{v}_{i-1} - \dot{v}_i - b_i \ddot{v}_i \Rightarrow \ddot{z}_i = \dot{v}_i = \ddot{z}_{i-1} - \ddot{\delta}_{iz} - b_i \dddot{z}_i \\
&\dddot{\delta}_{iz} = \ddot{v}_{i-1} - \ddot{v}_i - b_i \dddot{v}_i \Rightarrow \dddot{z}_i = v_i = \dddot{z}_{i-1} - \dddot{\delta}_{iz} - b_i \ddddot{z}_i.
\end{aligned} \tag{23}$$

The structure algorithm in Eq. 10 can be reformulated as follows:

$$\ddot{u}_{iz} = k_{1z} \ddot{z}_{iz} + k_{2z} \dddot{z}_i + k_{3z} \dot{\delta}_{iz} + k_{4z} \delta_{iz}. \tag{24}$$

Using these expressions in the car model in Eq. 3, λ is ignored for a flat road (no inclination):

$$\varsigma_v \ddot{z}_i + \dot{z}_i = K_v u_{iz}. \tag{25}$$

Replacing Eq. 23 into Eq. 25 results in:

$$(\varsigma_v \ddot{z}_{i-1} + \dot{z}_{i-1}) - b_i (\varsigma_v \dddot{z}_{i-1} + \ddot{z}_{i-1}) - K_v u_{iz} = \varsigma_v \ddot{\delta}_{iz} + K_v \dot{\delta}_{iz}. \tag{26}$$

After a simple calculation, it results:

$$K_v (\ddot{u}_{(i-1)z} - b_i \dddot{u}_{iz} - \ddot{u}_{iz}) = \ddddot{\delta}_{iz} + \dddot{\delta}_{iz}. \tag{27}$$

Bring Eq. 24 into Eq. 27,

$$\ddddot{\delta}_{iz} + \dddot{\delta}_{iz} = K_v (k_{1z} \ddot{\delta}_{iz} + k_{2z} \dddot{\delta}_{iz} + k_{3z} (\dot{\delta}_{(i-1)z} - \dot{\delta}_{iz} - b_i \ddot{\delta}_{iz}) + k_{4z} (\delta_{(i-1)z} - \delta_{iz} - b_i \dot{\delta}_{iz}). \tag{28}$$

By applying the unilateral Laplace transform to Eq. 28 under zero initial conditions – one obtain a closed-form spacing-error transfer function for the location-based ACC architecture. Eliminating the state variables in the transformed equations yields $\Xi_{iz}(s)$, which maps the predecessor's (or reference) position signal to the follower's spacing error. This representation provides the basis for subsequent frequency-response analysis and pole–zero inspection used to enforce the non-negativity and string-stability requirements.

$$\Xi_{iz}(s) := \frac{\delta_{iz}(s)}{\delta_{(i-1)z}(s)} = \frac{K_v k_{3z} s - K_v k_{4z}}{[\varsigma_v s^4 + (1 - K_v k_{2z}) s^3 + K_v (b_i k_{3z} - k_{iz}) s^2 - K_v (k_{3z} + b_i k_{4z}) s - K_v k_{4z}]}. \tag{29}$$

https://doi.org/10.14669/AM/210423

2.3.2. Stability analysis of ACC system based on distance

Using an analogous procedure to that adopted for the location-based ACC scheme, the spacing error can be formulated while incorporating the parameter b_i.

$$\delta_{iD} = r_0 + b_i v_i - D_i. \tag{30}$$

And subsequently, by differentiating both sides of Eq. 30 twice with respect to time, we obtain:

$$\begin{aligned}
&\dot{\delta}_{iD} = b_i \dot{v}_i - v_{i-1} + v_i \Rightarrow v_i = v_i = \dot{\delta}_{iD} + v_{i-1} - b_i \dot{v}_i \\
&\ddot{\delta}_{iD} = b_i \ddot{v}_i - \dot{v}_{i-1} + \dot{v}_i \Rightarrow \dot{v}_i = \ddot{\delta}_{iD} + \ddot{v}_{i-1} - b_i \ddot{v}_i \\
&\dddot{\delta}_{iD} = b_i \dddot{v}_i - \ddot{v}_{i-1} + \ddot{v}_i \Rightarrow \ddot{v}_i = v_i = \dddot{\delta}_{iD} + \dddot{v}_{i-1} - b_i \dddot{v}_i.
\end{aligned} \tag{31}$$

Using the relationship Eq. 3, here λ is ignored for a flat road (no inclination):

$$\varsigma_v \dot{v}_i + v_i = K_v u_{iz}. \tag{32}$$

Replacing Eq. 31 into Eq. 32 results in:

$$\varsigma_v \ddot{\delta}_{iD} + \dot{\delta}_{iD} = K_v (b_i \dot{u}_{iD} - u_{(i-1)D} + u_{iD}). \tag{33}$$

After a calculation, it results:

$$\begin{aligned}
&\varsigma_v \dddot{\delta}_{iD} + (1 - K_v k_{3D}) \ddot{\delta}_{iD} + K_v (k_{2D} - b_i k_{3D}) \ddot{\delta}_{iD} - K_v (k_{3D} + k_{4D} b_i) \dot{\delta}_{iD} - K_v k_{4D} \delta_{iD} \\
&= K_v k_{2D} \ddot{\delta}_{(i-1)D} - K_v k_{3D} \dot{\delta}_{(i-1)D} - K_v k_{4D} \delta_{(i-1)D}.
\end{aligned} \tag{34}$$

Finally, taking the unilateral Laplace transform of Eq. 34 under zero initial conditions – one can eliminate the state variables and obtain a closed-form transfer function for the spacing error between two successive cars in the spacing-based ACC architecture. The resulting expression where relevant) characterizes how inputs or disturbances associated with the predecessor car propagate to the follower's spacing error, and serves as the basis for the subsequent frequency-response and pole–zero analyses used to assess string stability.

$$\Xi_{iD}(s) := \frac{\delta_{iD}(s)}{\delta_{(i-1)D}(s)} = \frac{K_v k_{2D} s^2 - K_v k_{3D} s - K_v k_{4D}}{[\varsigma_v s^4 + (1 - K_v k_{3D}) s^3 + K_v (k_{2D} - b_i k_{3D}) s^2 - K_v (k_{3D} + b_i k_{4D}) s - K_v k_{4D}]}. \tag{35}$$

3. Results and discussion

Numerical simulations were conducted to analyze the performance of an autonomous cars homogeneous platoon. Two ACC configurations, namely location-based and spacing-based, were considered along with the CTHP method. The platoon consists of 13 homogeneous car, with the first car acting as the leader and the next 12 cars functioning as followers. The vehicle

https://doi.org/10.14669/AM/210423

dynamics were represented using the transfer function in Eq. 3, with model parameters taken from [21]. Specifically, the amplification coefficient was set to $K_v = 0.075$ and the associated time constant was $\varsigma_v = 75.6s$.

The lead car is governed by a velocity control system employing a CC-PID controller. Each following car maintains a specified gap from the car ahead, utilizing one of two ACC control strategies. Accordingly, the gain matrix K_{iz} of the LQI²R controller (as specified in Eq. 10) is determined for the location-based ACC setup, while the matrix for the controller described in Eq. 17 is used for the spacing-based ACC configuration.

The spacing-error transfer functions were first constructed by substituting the prescribed matrices into Eqs. 29 and 35. In particular, the state-feedback gain vectors used in the derivation were K_{iz} = [-6846.8 -4181.5 5573.8 1974.9], K_{iD} = [6841 -4181.5 -5573.5 -1974.9]. Injecting these gains into the formulas yields explicit expressions for the spacing-error transfer functions, which then serve as the basis for the subsequent frequency-response evaluation and pole–zero analysis used to assess string stability.

String stability analysis of the spacing errors for two consecutive cars, as described by Eq. 29, Eq. 35 involves using the string stability conditions from Eq. 19. These conditions are examined by plotting the magnitude frequency, as shown in Figure 5, Figure 6, while increasing b_i from 0.65s to 2.6s.

For the spacing-based ACC configuration, the platoon of cars with b_i = [0.65s; 0.9s; 1.5s; 2.6s], are robust string stability as the corresponding the maximum magnitude is equal to or less than the value 1, as in Figure 5. In contrast, for the location-based ACC configuration, the maximum magnitude as in Figure 6, the time headway b_i was incrementally increased until b_i = 2.6s, at which stability was achieved. We can see that the time headway is incrementally increased with different values b_i = [0.65s; 0.9s; 1.5s], the stability condition (20) is not satisfied ("weak stability") as the maximum magnitude is exceed 1, the system is only stable with b_i = 2.6s.

The result indicates that the spacing-based ACC structure will have a much smaller steady-state distance value b_i, which is an advantage compared to the distance-based ACC structure. To verify this, spacing errors δ_i for the ith car in a platoon were observed.

The evaluation of string stability was performed using the interconnected platoon simulator, which follows the configuration shown in Figure 2. The simulation considered a convoy of n = 13 cars, with each car length l_i = 5m and standstill spacing r_0 = 2m To assess performance, the spacing errors δ_i were plotted and examined. The test scenario began with the lead vehicle held at rest for 120 seconds to allow the platoon to reach equilibrium, after which a step input in the speed reference of v_{ref} of 23 m/s was applied to the system.

https://doi.org/10.14669/AM/210423

The spacing errors for the spacing-based ACC configuration with a time headway of $b_i = 0.65$s are shown in Figure 7, it illustrates that spacing errors for two consecutive cars are bounded and decrease along the platoon, indicating robust string stability. Similarly, for the location-based ACC configuration, the spacing errors are depicted in Figure 8, as spacing errors become increasingly amplified, the followers will gradually lose control and diverge from the trajectory of the platoon leader.

Achieving robust string stability requires the system's impulse response to remain non-negative, thereby avoiding oscillatory sign changes that could amplify along the platoon. In practice, this constraint is enforced by satisfying two pole-zero conditions. Those conditions act as a design filter on the controller gains and time headway: they exclude configurations whose dynamics would introduce undershoot or peaking, and retain only transfer functions whose transient behavior is monotone and thus compatible with string-stable propagation of disturbances.

To determine the value of b_i that satisfies the stability criterion (can see in subsection 2.3), it is necessary to examine the pole-zero maps of both $\Xi_{iz}(s)$, $\Xi_{iD}(s)$ while sweeping b_i from $b_i = 0.65$s to $b_i = 6.6$s (Figures 9–10). The plots show that the condition required for a non-negative impulse response is not fulfilled until $b_i = 6.6$s. For smaller b_i, the dominant closed-loop poles appear as a complex-conjugate pair, which implies oscillatory transients and sign changes in the impulse response. When b_i reaches 6.6s, these dominant poles move onto the real axis, yielding a monotone response that satisfies the non-negativity requirement. Under this setting, string stability is achieved only for the location-based ACC configuration, whose transfer function features a single real negative zero. In contrast, the spacing-based ACC configuration does not satisfy Eq. 21 for any choice of b_i, because a complex-conjugate pair of zeros in its transfer function prevents the non-negative impulse-response condition from being met.

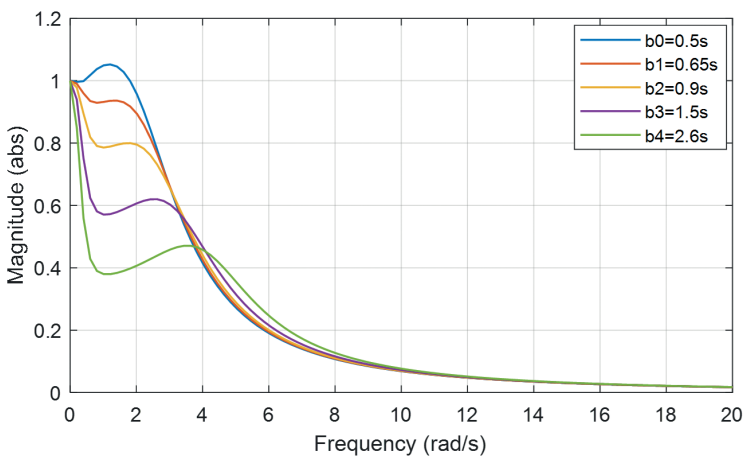

Fig. 5. String stability plots based on distance with different values of headway time b_i

https://doi.org/10.14669/AM/210423

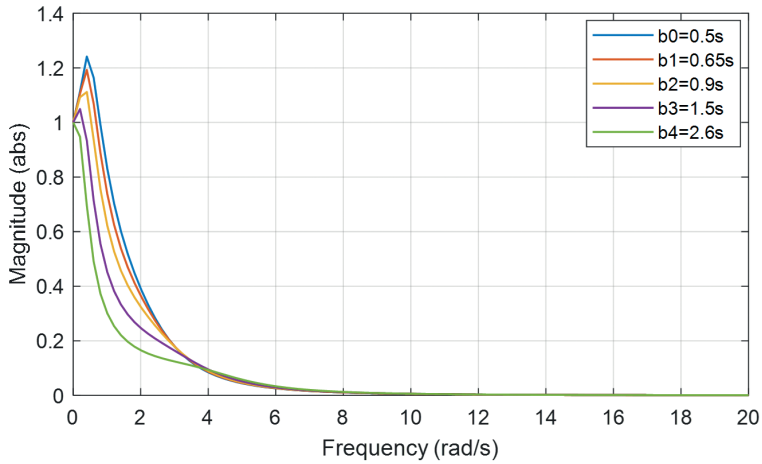

Fig. 6. String stability plots based on location with different values of headway time b_i

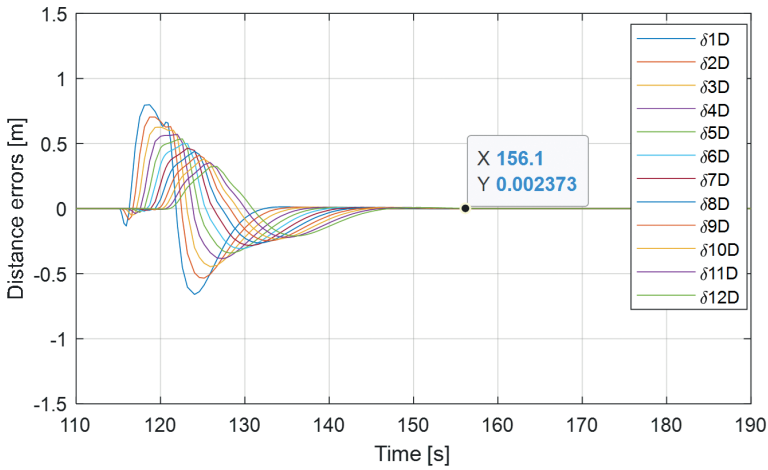

Fig. 7. Simulation result of spacing errors based on distance $b_i = 0.65s$

https://doi.org/10.14669/AM/210423

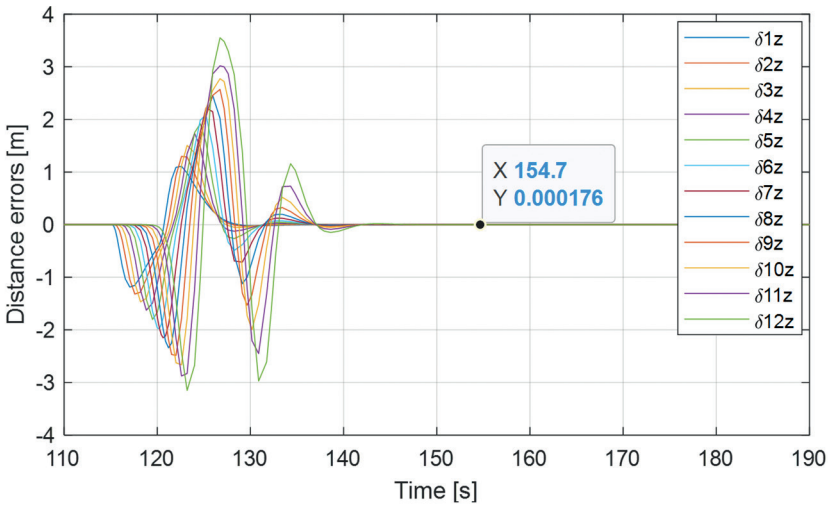

Fig. 8. Simulation result of spacing errors based on location $b_i = 0.65s$

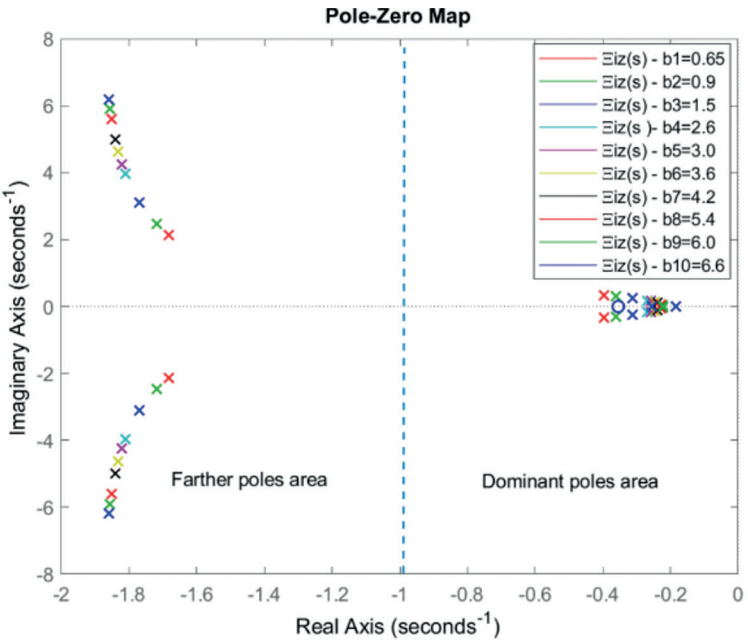

Fig. 9. Transfer function analysis $\Xi_{iz}(s)$ based on location: Pole-zero mapping

https://doi.org/10.14669/AM/210423

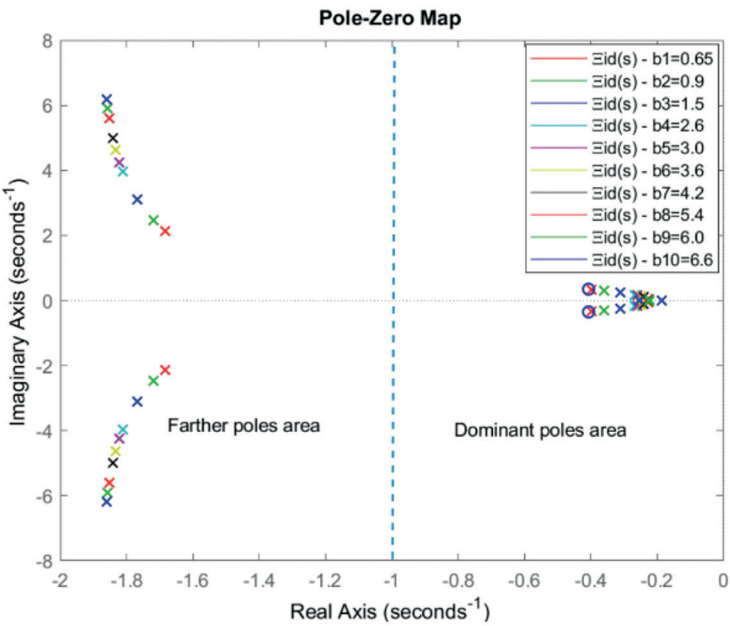

Fig. 10. Transfer function analysis $\Xi_{iD}(s)$ based on distance: Pole-zero mapping

4. Conclusions

This study investigates the synthesis of an LQI²R controller for vehicle platoons operating under ACC. The design target is twofold: attain accurate reference tracking at the individual-vehicle level and, simultaneously, guarantee string stability – i.e., prevent disturbances introduced by one vehicle from amplifying as they propagate along the convoy. To meet the latter requirement, we propose a pragmatic, transfer-function–driven tuning routine centered on the spacing-error dynamics. The routine proceeds in two coordinated stages. First, an appropriate time headway is selected by examining the frequency response of the spacing-error transfer function and choosing a value that limits the gain across the frequency band of interest, thereby curbing disturbance growth. Second, this choice is vetted against the pole–zero portrait of the resulting closed-loop transfer function to ensure favorable damping, left-half-plane pole placement, and the absence of problematic pole–zero interactions that would compromise robustness. The LQI²R controller is instantiated for two ACC formulations: one that leverages absolute position (location-based feedback) and another that relies on inter-vehicle distance (spacing-based feedback). A comparative evaluation of platoon string stability under these two configurations is then conducted in simulation, using the proposed heuristic as the common design and assessment framework.

5. References

[1] Aron C, Florin M. Current approaches in traffic lane detection: a minireview. The Archives of Automotive Engineering – Archiwum Motoryzacji. 2024;104(2):19–47. https://doi.org/10.14669/AM/190157.

[2] Mohammed D, Nagy V, Jagicza M, Józsa D, Horváth B. Efficiency of adaptive cruise control in commercial vehicles. Pollack Periodica. 2024;19(2):1–7. https://doi.org/10.1556/606.2024.00970.

[3] Li Y, Zhang W, Zhang S, Pan Y, Zhou B, Jiao S, et al. An improved eco-driving strategy for mixed platoons of autonomous and human-driven vehicles. Physica A: Statistical Mechanics and its Applications. 2024;641:129733. https://doi.org/10.1016/j.physa.2024.129733.

[4] Pan C, Huang A, Chen L, Cai Y, Chen L, Liang J, et al. A review of the development trend of adaptive cruise control for ecological driving. Proceedings of the Institution of Mechanical Engineers, Part D: Journal of Automobile Engineering. 2022; 236(9):1931–1948. https://doi.org/10.1177/09544070211049068.

[5] Yang J, Chu D, Lu L, Meng Z, Deng K. Model-data-driven control for human-leading vehicle platoon. Proceedings of the Institution of Mechanical Engineers, Part D: Journal of Automobile Engineering. 2025;239(7):2616–2636. https://doi.org/10.1177/09544070241240037.

[6] Zainuddin MA, Abdullah M, Ahmad S, Tofrowaih KA. Performance comparison between predictive functional control and PID algorithms for automobile cruise control system. International Journal of Automotive and Mechanical Engineering. 2022;19(1):9460–9468. https://doi.org/10.15282/ijame.19.1.2022.09.0728.

[7] Abdullah SI, Zainuddin MA, Abdullah M, Tofrowaih KA. Analysis of a Simplified Predictive Function Control Formulation Using First Order Transfer Function for Adaptive Cruise Control. International Journal of Automotive and Mechanical Engineering. 2024;21(3):11641–11651. https://doi.org/10.15282/ijame.21.3.2024.15.0898.

[8] Zainuddin MA, Abdullah M, Ahmad S, Uzir MS, Baidowi ZM. Performance analysis of predictive functional control for automobile adaptive cruise control system. IIUM Engineering Journal. 2023;24(1):213–225. https://doi.org/10.31436/iiumej.v24i1.2341.

[9] Shang M, Stern RE. Impacts of commercially available adaptive cruise control vehicles on highway stability and throughput. Transportation research part C: Emerging technologies. 2021;122:102897. https://doi.org/10.1016/j.trc.2020.102897.

[10] Gunter G, Gloudemans D, Stern RE, McQuade S, Bhadani R, Bunting M, et al. Are commercially implemented adaptive cruise control systems string stable?. IEEE Transactions on Intelligent Transportation Systems. 2020;22(11):6992–7003. https://10.1109/TITS.2020.3000682.

[11] Zhang Y, Bai Y, Hu J, Wang M. Control design, stability analysis, and traffic flow implications for cooperative adaptive cruise control systems with compensation of communication delay. Transportation Research Record. 2020;2674(8):638–652. https://doi.org/10.1177/0361198120918873.

[12] Abdullah M, Zainuddin MS, Ahmad S, Rossiter J. Performance comparison between centralized and hierarchical predictive functional control for adaptive cruise control application. International Journal of Automotive and Mechanical Engineering. 2023;20(4):10808–10820. https://doi.org/10.15282/ijame.20.4.2023.01.0836.

[13] Chen Q, Gan L, Jiang Z, Xu Z, Zhang X. Study on multi-objective adaptive cruise control of intelligent vehicle based on multi-mode switching. Proceedings of the Institution of Mechanical Engineers, Part D: Journal of Automobile Engineering. 2024;238(14):4505–4517. https://doi.org/10.1177/09544070231198278.

[14] Luo L, Liu Y, Feng Y, Liu HX, Ge YE. Stabilizing traffic flow by autonomous vehicles: Stability analysis and implementation considerations. Transportation research part C: Emerging technologies. 2024;158:104449. https://doi.org/10.1016/j.trc.2023.104449.

[15] Luu L, Phan TL, Pham HT, Hoang T, Le MT. Stability of adaptive cruise control of automated vehicle platoon under constant time headway policy. International Journal of Automotive Science and Technology. 2024;8(3):397–403. https://doi.org/10.30939/ijastech..1469674.

[16] Darbha S, Konduri S, Pagilla PR. Benefits of V2V communication for autonomous and connected vehicles. IEEE Transactions on Intelligent Transportation Systems. 2019;20(5):1954–1963. https://doi.org/10.1109/TITS.2018.2859765.

[17] Abolfazli E, Besselink B, Charalambous T. Minimum time headway in platooning systems under the MPF topology for different wireless communication scenario. IEEE Transactions on Intelligent Transportation Systems. 2023;24(4):4377–4390. https://doi.org/10.1109/TITS.2023.3239655.

[18] Köroğlu H. String-stable cooperative adaptive cruise control with minimized time headway in the face of delayed communication. IEEE Control Systems Letters. 2024;8:400–405. https://doi.org/10.1109/LCSYS.2024.3392716.

[19] Lu XY, Shladover S. Integrated ACC and CACC development for heavy-duty truck partial automation. Proceedings of the American Control Conference. 2017:4938–4945. https://doi.org/10.23919/ACC.2017.7963720.

[20] Bian Y, Zheng Y, Ren W, Li SE, Wang J, Li K. Reducing time headway for platooning of connected vehicles via V2V communication. Transportation Research Part C: Emerging Technologies. 2019;102:87–105. https://doi.org/10.1016/j.trc.2019.03.002.

[21] Ibrahim A, Goswami D, Li H, Soroa IM, Basten T. Multi-layer multi-rate model predictive control for vehicle platooning under IEEE 802.11p. Transportation Research Part C: Emerging Technologies. 2021;124:102905. https://doi.org/10.1016/j.trc.2020.102905.

[22] Wu C, Xu Z, Liu Y, Fu C, Li K, Hu M. Spacing policies for adaptive cruise control: A survey. IEEE Access. 2020;8:50149–50162. https://doi.org/10.1109/ACCESS.2020.2978244.